Research article

Microglial ROS production in an electrical rat post-status epilepticus model of epileptogenesis

Maruja L. Rettenbeck [a,1], Eva-Lotta von Rüden [a,1], Silvia Bienas [b], Regina Carlson [b], Veronika M. Stein [b], Andrea Tipold [b], Heidrun Potschka [a,*]

[a] Institute of Pharmacology, Toxicology, and Pharmacy, Ludwig-Maximilians-University, Munich, Germany
[b] Department of Small Animal Medicine and Surgery, University of Veterinary Medicine Hannover, Hannover, Germany

HIGHLIGHTS

- Epileptogenesis-associated microglial ROS generation is altered in an electrical post-SE model.
- Excessive generation of microglial ROS was demonstrated in the early post-SE phase.
- Moderate generation of microglial ROS was detected in the latency phase.
- Microglial ROS generation returned to control levels in the chronic epileptic phase.
- Radical scavenging approaches might only be beneficial shortly after the initial insult.

ARTICLE INFO

ABSTRACT

Reactive oxygen species and inflammatory signaling have been identified as pivotal pathophysiological factors contributing to epileptogenesis. Considering the development of combined anti-inflammatory and antioxidant treatment strategies with antiepileptogenic potential, a characterization of the time course of microglial reactive oxygen species generation during epileptogenesis is of major interest. Thus, we isolated microglia cells and analyzed the generation of reactive oxygen species by flow cytometric analysis in an electrical rat post-status epilepticus model.

Two days post status epilepticus, a large-sized cell cluster exhibited a pronounced response with excessive production of reactive oxygen species upon stimulation with phorbol-myristate-acetate. Neither in the latency phase nor in the chronic phase with spontaneous seizures a comparable cell population with induction of reactive oxygen species was identified.

We were able to demonstrate in the electrical rat post-status-epilepticus model, that microglial ROS generation reaches a peak after the initial insult, is only marginally increased in the latency phase, and returns to control levels during the chronic epileptic phase. The data suggest that a combination of anti-inflammatory and radical scavenging approaches might only be beneficial during a short time window after an epileptogenic brain insult.

1. Introduction

Experimental and clinical research indicates that inflammatory signaling and oxidative stress can significantly contribute to epileptogenesis following brain insults [1,2]. Oxidative stress induced by excitotoxicity and neuronal death results in the production of reactive oxygen species (ROS) leading to an imbalance of oxidant production and antioxidant defense. Therefore, ROS is discussed as a key pathophysiological mechanism not only occurring after the brain insult but also contributing to epileptogenesis [1]. However, there is limited knowledge about ROS generation in acquired epilepsies including temporal lobe epilepsy (TLE) and during epileptogenesis as well as about the time course of ROS production generated by specific cell types such as microglia cells. During pathological insults, microglia cells thicken, retract their processes, proliferate, migrate and release several factors, like ROS [3].

* Corresponding author at: Institute of Pharmacology, Toxicology, and Pharmacy, Ludwig–Maximilians–University, Koeniginstr. 16, D–80539 Munich, Germany. Tel.: +49 89 21802662; fax: +49 89 2180 16556.
E-mail address: potschka@pharmtox.vetmed.uni-muenchen.de (H. Potschka).
[1] Both authors contributed equally to this work.

Anti-inflammatory and antioxidant strategies are intensely evaluated in rodent models of epilepsy [4,5]. Therefore, the identification of the time course of microglial ROS generation is critical for the development of rational pharmacological intervention strategies targeting oxidative stress and inflammation.

Seizure-associated stimulation of free radicals has been reported in some animal models following exposure to chemoconvulsants like kainic acid [5–9]. Considering that it is impossible to distinguish between direct effects of the chemoconvulsant and epileptogenesis-associated alterations in chemical epilepsy models, available data are difficult to interpret. Thus, we decided to perform a thorough functional analysis of the course of microglial ROS generation in an electrical rat post-status epilepticus (SE) model with stimulation of the basolateral amygdala to exclude this bias.

Functional analysis of microglial ROS production is possible based on exposure of freshly isolated cells to chemical stimuli and assessment of the response. For instance, the generation of ROS can be evaluated in response to phorbol-myristate-acetate (PMA) stimulation [10,11] followed by flow cytometric analysis. Based on the fact, that the time course of microglial responsiveness and ROS generation is of particular relevance for the identification of time windows for intervention strategies, we have isolated microglia cells and applied a flow cytometric analysis to elucidate the course of epileptogenesis-associated ROS alterations in an electrical rat post-SE model with development of spontaneous recurrent seizures (SRS). The results of our study may render a basis for future assessment of antiepileptogenic approaches targeting inflammation along with oxidative stress.

2. Material and methods

2.1. Animals and animal model

Female Sprague Dawley rats were purchased at a bodyweight of 200–224 g (Harlan, Udine, Italy). The experiments were performed in compliance with the European Union directive 2010/63/EU for animal experiments and with the German Animal Welfare act. Experiments were approved by the Government of Upper Bavaria and Lower Saxony (license number 55.2-1-54-2532-173-11). All efforts were made to decrease pain or discomfort of the animals used in the experiment.

Fig. 1A gives a schematic timeline of the study design. A depth electrode was implanted into the right basolateral amygdala (stereotactic coordinates in millimeters relative to Bregma: ap −2.2, ll + 4.7, dv −8.5) of female Sprague Dawley rats (n = 164) as described earlier [12]. A self-sustained SE was induced (n = 78) by electrical stimulation as described previously [13]. Animals were grouped as follows: (1) two days post SE, (2) ten days post SE (group 1. and group 2.: only rats, which developed a type III self-sustained status epilepticus (four hours of continuous generalized seizure activity)) and (3) twelve weeks post SE (only rats with SRS). The rats from the chronic phase underwent a three week video- and EEG-monitoring as described elsewhere (24 h/7 days per week) [13,14]. Animals were deeply anesthetized with pentobarbital (500 mg/kg, i.p.; Narkodorm®, cp-Pharma, Burgdorf, Germany) and perfused transcardially with ice cold electrolyte solution (Sterofundin®, Braun, Melsungen, Germany) two days (= acute phase), ten days (= latency phase), and twelve weeks (= chronic phase) following SE.

2.2. Isolation of microglial cells

After perfusion microglial cells were isolated by density gradient centrifugation (see Fig. 1) and *ex-vivo* studies were performed as described by Stein et al. [11]. Cells were collected from the interface between the density layers of 1.066 g/ml and 1.077 g/ml (Percoll; GE Healthcare, Freiburg, Germany). Absolute number of cells and cell viability were determined directly afterwards by trypan blue staining (Sigma–Aldrich GmbH, Steinheim, Germany).

Pilot experiments revealed that it is necessary to pool three brains from control or SE animals to gain sufficient cell numbers for subsequent microglia analysis. Limitations in the cell yield per preparation result from the age of the animals in the chronic epilepsy model.

2.3. Immunophenotyping

Microglial cells were identified based on their expression profile of CD18$^+$, CD11b$^+$ and CD45^{low} in combination with the parameters size and complexity [3,11,15–19].

After determining the absolute number of cells, microglial cells were stained with directly labeled mouse monoclonal antibodies against CD45-AF 647, CD11b-FITC, CD18-FITC and CD3-AF 647. Flow cytometry was performed using a FACSCalibur™ (Becton Dickinson, Heidelberg, Germany) as described by Stein et al. [11]. Microglia were analyzed using CellQuest Pro™-Software (version 5.2.1, Becton Dickinson, Franklin Lakes, New Jersey, USA, for Apple & Macintosh®).

2.4. ROS generation test

ROS generation by microglial cells was assessed by a method described earlier by Stein et al. [11]. Briefly, dihydrorhodamine 123 (DHR 123, MoBiTec GmbH, Göttingen, Germany) was diluted in dimethylsulfoxide (DMSO, Sigma-Aldrich GmbH, Steinheim, Germany) in a concentration of 15 μg/ml. The stimulans phorbol-myristate-actetate (PMA, Sigma–Aldrich GmbH, Steinheim, Germany) was diluted in DMSO and further diluted with phosphate buffered saline (PBS) to a final concentration of 100 nmol. The ROS generation test was performed in duplicates for each approach. Ninety μl of the cell suspension were pre-incubated for 15 min at 37 °C and 5% CO_2, then incubated with 10 μl PMA or 10 μl PBS (negative control) followed by DHR 123 incubation under the same conditions. To terminate the ROS generation, cells were stored on ice for 15 min in the dark. Immediately afterwards, cells were measured.

2.5. Statistical analysis

We performed statistical analysis of group differences using Graph Pad Prism (version 5.04, GraphPad-San Diego, CA, USA). All data are given as mean ± SEM. One-way analysis (ANOVA) followed by a Bonferroni's Multiple Comparison Test was used for calculation of intergroup differences. Direct comparison of rats with SE and electrode-implanted controls was performed by the Student's t-test with or without Welch's correction. The Pearson correlation coefficient was determined to test for a correlation between seizure frequency and microglial ROS generation. A p value of <0.05 was considered statistically significant.

3. Results

3.1. Purity of the ex-vivo cell yield

Cell yields varied from 1.0×10^6 to 2.4×10^6 total viable cells in electrode-implanted control animals and from 0.8×10^6 to 2.8×10^6 in SE animals per 5.3–6.6 g brain tissue. A ToPro-3 staining distinguished living from dead cells via FACS analysis. Viable cells were used for further *ex-vivo* analysis.
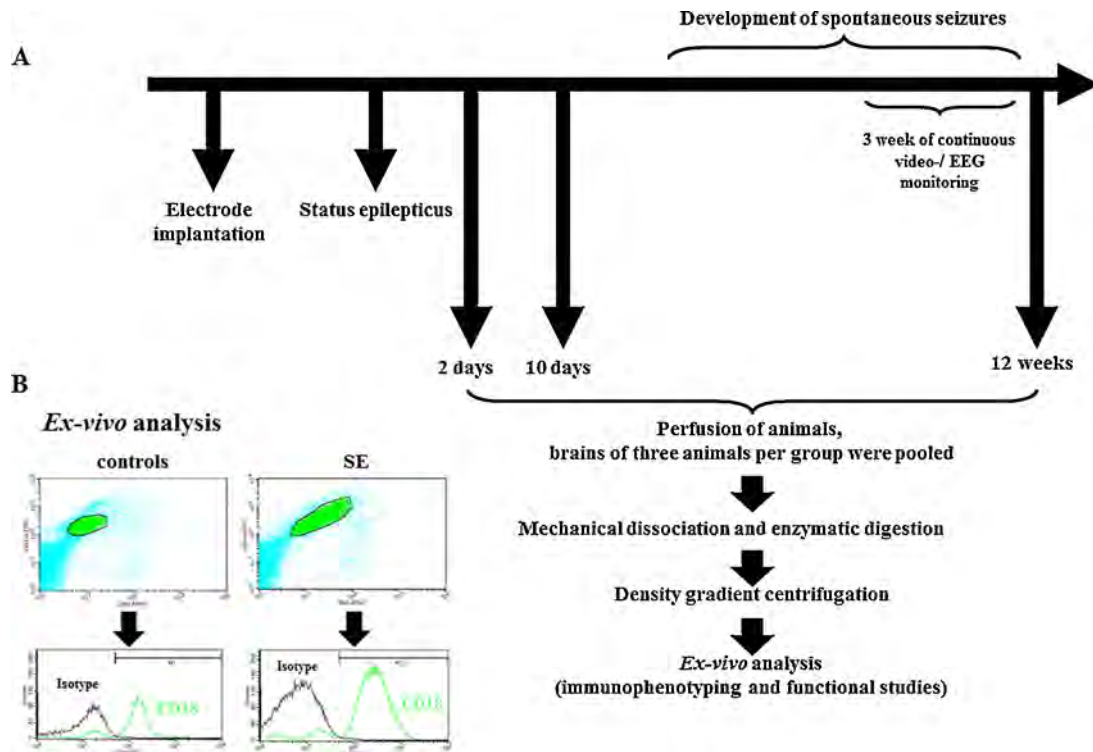
Fig. 1. Experimental design (A) and procedure of *ex-vivo* analysis (B).
Microglial cells were depicted in a dot plot representing co-expression of CD11b and CD45^{low}. These cells were used for further *ex-vivo* examination.

Cells co-expressing CD11b and CD45^{low} were considered microglia cells (Fig. 1B). These cells were gated and displayed in a dot plot for size and complexity, in which they formed a homogenous cell cluster. Only cells within this gate were used for further analysis.

The purity of isolated microglia cells was controlled based on the CD11b and CD18 expression profile (Suppl. Table 1). The percentage of CD18$^+$ cells ranged from 72% to 92% in electrode-implanted control animals and from 30% to 94% in SE animals (Suppl. Table 1). CD3 was used to determine a contamination with T-lymphocytes. A low T-cell contamination of less than 2% was evident.

3.2. Two days post SE isolated cells generated ROS upon stimulation

The analysis of ROS generation upon stimulation with PMA was performed considering different cell populations from electrode-implanted controls and SE animals (Fig. 2). Respective cell populations were selected based on clustering of cells in the parameters size and complexity. In electrode-implanted controls, a small- and a medium-sized cell cluster were evident in samples obtained from all three time points (Fig. 2A–C). Basal ROS levels of the small-sized cell clusters proved to be elevated in SE animals two and ten days following the epileptic insult (two days $p_{PBS} = 0.03$ and ten days $p_{PBS} = 0.02$, Table 1).

In control animals, the small- and medium-sized cell clusters differed in their basal levels of ROS generation with a higher level in the medium-sized cell clusters compared to the small-sized cell clusters (two days $p_{PBS} < 0.05$, ten days $p_{PBS} < 0.05$, 12 weeks $p_{PBS} < 0.05$, Table 1). In line with these findings, the response to PMA in the medium-sized cell clusters exceeded that in the small-sized cell clusters (two days $p_{PMA} < 0.05$, ten days $p_{PMA} < 0.05$, twelve weeks $p_{PMA} < 0.05$, Table 1). No increase was observed in response to PMA stimulation in electrode implanted controls (two days

$p_{small} = 1.0$, $p_{medium} = 0.08$, Fig. 2G and Table 1; ten days $p_{small} = 0.4$, $p_{medium} = 0.6$; twelve weeks $p_{small} = 0.8$, $p_{medium} = 0.2$, Table 1).

Two days post SE three cell clusters (small-, medium- and large-sized) were identified (Fig. 2D). The large-sized cell clusters were characterized by a higher complexity as compared to the smaller cell clusters. These three cell clusters also exhibited different basal levels of ROS generation with the highest basal level evident in the large-sized cell cluster (two days $p_{PBS,small\ vs\ medium} < 0.05$, $p_{PBS,medium\ vs\ large} < 0.05$, Table 1). The mean ROS generation intensity from PBS-treated cells ranged from 5.7 to 21.0 in the small-, from 29.0 to 58.6 in the medium-sized, and from 62.5 to 122.0 in the large-sized cell population. The mean ROS generation intensity from PMA treated cells in the large-sized cell clusters ranged from 72.0 to 314.0. Neither the small- nor the medium-sized cell clusters exhibited any relevant response to PMA stimulation ($p = 0.4$ and $p = 0.4$, respectively, Fig. 2H and Table 1). In apparent contrast, ROS generation increased in a significant manner upon PMA exposure in the large-sized cell population ($p = 0.0495$, Fig. 2H and Table 1).

Ten days and twelve weeks post SE, cell clustering according to size and complexity proved to be comparable with that in electrode-implanted controls (Fig. 2 E and F). Ten days post SE the mean ROS generation intensity of PBS-treated cells ranged from 6.1 to 12.7 in the small- and from 42.0 to 90.5 in the medium-sized cell clusters. Twelve weeks post SE the mean ROS generation intensity of PBS-treated cells ranged from 6.7 to 10.9 in the small- and from 43.4 to 59.5 in the medium-sized cell clusters.

Neither the small- nor the medium-sized cell populations increased ROS generation upon PMA stimulation at these time points (ten days post SE $p_{small} = 0.3$, $p_{medium} = 0.2$; twelve weeks post SE $p_{small} = 0.8$, $p_{medium} = 0.06$, Table 1). However, ten days following SE the small-sized cell clusters in SE animals showed an increased intensity of ROS generation compared to control animals ($p_{PBS} = 0.02$, $p_{PMA} = 0.01$; Table 1).

There was no correlation between the seizure frequency (range 1–109 during the three weeks of video-/EEG-monitoring) and the

Table 1
ROS generation intensity of the different cell clusters.

	Reactive oxygen species – mean fluorescence intensity (geo mean)											
	2 Days post SE				10 Days post SE				12 Weeks post SE			
	Control $\bar{x} \pm$ SEM		SE $\bar{x} \pm$ SEM		Controls $\bar{x} \pm$ SEM		SE $\bar{x} \pm$ SEM		Controls $\bar{x} \pm$ SEM		SE $\bar{x} \pm$ SEM	
	PBS	PMA	PBS	PMA	PBS	PMA	PBS	PMA	PBS	PMA	PBS	PMA
Small-sized cell cluster	6.6 ± 0.3[a]	6.6 ± 0.2[a]	10.9 ± 1.6[h]	16.7 ± 5.9	7.1 ± 0.3[a]	6.8 ± 0.2[a]	9.6 ± 0.8[a,g,h]	8.6 ± 0.5[a,g]	9.3 ± 1.0	9.0 ± 0.6	8.5 ± 0.4	8.7 ± 0.2
Medium-sized cell cluster	43.6 ± 1.7[c]	48.5 ± 2.0[d]	42.7 ± 3.4[c]	55.9 ± 14.3	45.7 ± 2.4[c]	48.0 ± 3.0[d]	56.0 ± 4.9[c]	48.9 ± 3.1[d]	49.2 ± 2.8[c]	54.6 ± 2.5[d]	49.0 ± 1.7[c]	53.3 ± 1.3[d]
Large-sized cell cluster			90.3 ± 6.1[e]	153.2 ± 27.1[b,f]								

SE = Status epilepticus; PBS = phosphate buffered saline; PMA = phorbol-myristate-acetate; $\bar{x} \pm$ SEM = mean ± standard error of the mean; means are calculated from 5 repetitive experiments, ROS generation tests were performed in duplicates for each approach;

[a] Mean calculated from 4 repetitive experiments;
[b] Significant difference between PBS and PMA treated cells in the large-sized cell cluster;
[c] Significant difference between small- and medium-sized cell clusters (PBS);
[d] Significant difference between small- and medium-sized cell clusters (PMA);
[e] Significant difference between medium- and large-sized cell clusters (PBS);
[f] Significant difference between medium- and large-sized cell clusters (PMA);
[g] Ten days post SE the small-sized cell cluster in SE animals showed an increased intensity of ROS generation compared to control animals (PBS and PMA);
[h] Significant difference between PBS treated cells in control and SE animals.

respective ROS generation intensities in the chronic phase (Pearson $r = 0.035$, $p = 0.569$; Suppl. Table 2).

In summary, our results point toward excessive generation of microglial ROS generation at two days post SE, and only marginally increased ROS generation at ten days post SE. At twelve weeks post SE ROS generation returned to control levels.
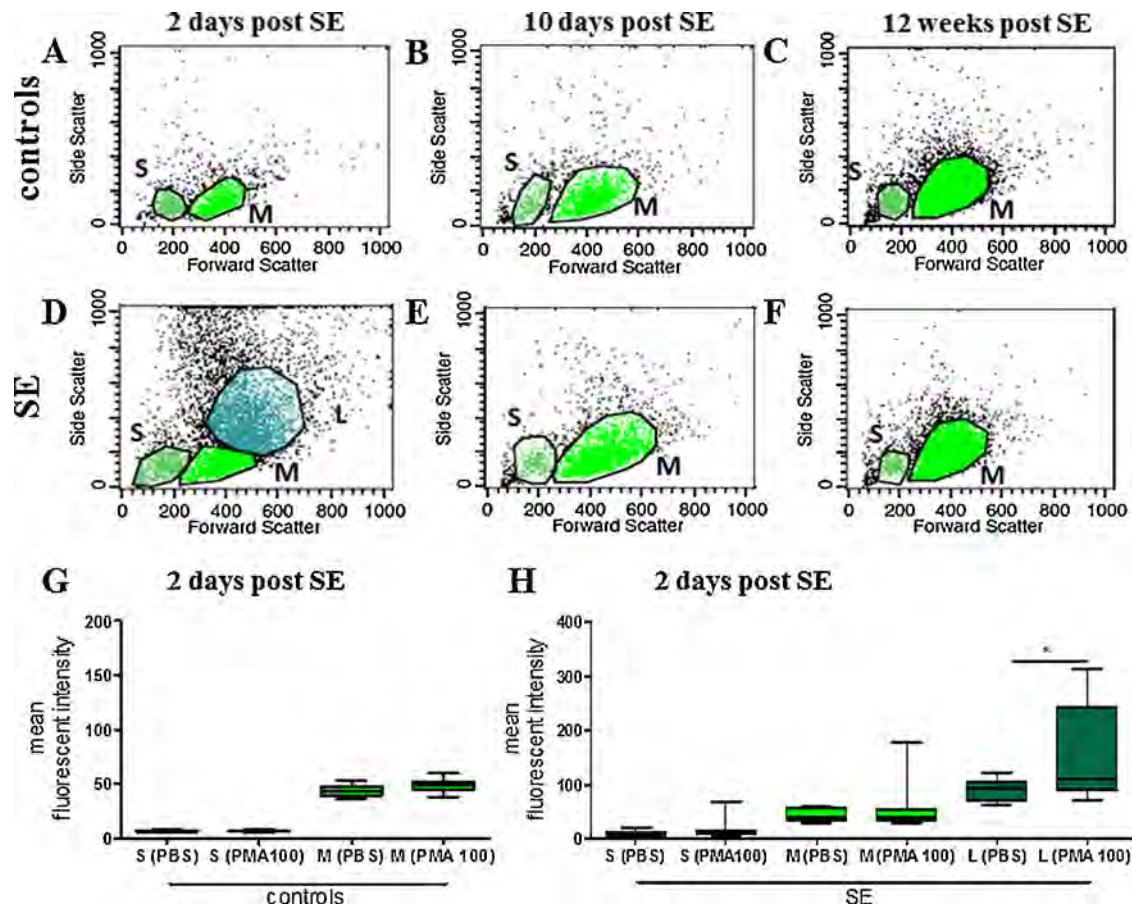

Fig. 2. Time course of ROS generating cell populations in electrode-implanted controls (A–C) and in SE animals (D–F).
Two days, ten days and twelve weeks post SE (A–F) a small- and a medium-sized ROS generating cell population were identified. (D) Two days post SE an additional large-sized ROS generating cell population was identified. Quantitative analysis of ROS generation: (G) No increase of ROS generation upon PMA stimulation. (H) The large-sized cell population produced ROS upon stimulation.
PBS = phosphate buffered saline; PMA = phorbol-myristate-acetate; S = small-sized cell population, M = medium-sized cell population, L = large-sized cell population. All data are given as mean ± SEM; $p < 0.05$; (*) significant difference upon PBS (negative control) and PMA stimulation.

4. Discussion

Oxidative stress has been described as a factor that does not only occur acutely as a result of a precipitating injury but also during epileptogenesis and in the chronic epileptic brain [1,5,8,20–22]. Therefore, we evaluated the alterations of microglial ROS generation in the course of epileptogenesis in an electrical post-SE model avoiding a putative chemoconvulsant-associated bias.

We determined basal microglial ROS generation and upon cell stimulation with PMA. PMA is a strong stimulator of ROS production, which has been repeatedly used in experiments assessing ROS generation activities of microglia cells [10,11,23]. Basal ROS levels proved to be elevated in SE animals two and ten days following the epileptic insult and a pronounced ROS generation was evident following PMA exposure of one cell population isolated from animals two days following SE. In the chronic phase ROS levels returned to control levels. The early finding is in line with the study of Sleven et al. [24], who found reduced glutathione levels in an electrically-induced limbic SE model up to 44 h after SE and suggested that reduction of oxidative stress following the insult might help to prevent pathological consequences of SE. However, the question about the long-term course during epileptogenesis remained to be further addressed.

A similar time course of ROS generation was evident in the kainic acid model of epilepsy [9,25]. In contrast, a pilocarpine-induced SE resulted in an early ROS peak followed by a sustained increase of ROS levels during the latency and chronic period [25]. When comparing the findings from different studies, the incidence of SRS development for the respective epilepsy model needs to be considered. While in the kainic acid model <50% of the treated animals might develop SRS, the pilocarpine model reliably results in SRS in almost all rats [26]. Unfortunately, Dal-Pizzol et al. [25] did not monitor if experimental animals developed SRS. Therefore, it cannot be excluded that animals without SRS are included in their analysis. In our hands, all animals representing the chronic epileptic phase exhibited SRS in the course of the experiment. However, a rather low to moderate seizure frequency is typical for the electrical post-SE model. Our findings suggest that the low seizure density does not trigger a sustained increase in ROS generation in the chronic phase. We cannot exclude that in a model with high SRS frequency ROS generation is increased. Moreover, the technique might be appropriate for the assessment of microglial ROS generations during the early phase and the latency phase of epileptogenesis, but might lack sensitivity to determine more subtle chronic activation patterns in the phase with SRS.

Depending on the cellular localization ROS have physiological as well as pathological roles in the brain [1,27]. Here, we analyzed microglial ROS production and demonstrated an early peak of ROS following the initial brain insult. Microglia cells are strongly activated in this phase related to pronounced neuronal death and release of danger-associated molecular pattern molecules such as HMGB1 [2,28]. Thus, the transient increase in microglia responsiveness and ROS generation might reflect the time course of neuronal damage, which has been repeatedly described in the hippocampus and other regions of the temporal lobe in the early phase following electrically induced SE. Neuronal death associated with the effects of oxidative damage may lead to the progressive nature of epileptogenesis and the long-term pathological effects [29]. This seems to be reasonable not only for mature but also for immature animals and might be linked to an inhibition of the mitochondrial complex I [30].

It is well known that macrophages are larger than microglia cells and generate higher levels of ROS [11]. Moreover, microglia cells display a morphological polymorphism [3,31,32]. The different cell sizes and phenotypes of microglia cells are reflected by different cell clusters referring to size and complexity of the cells in the FACS analysis. Here, we observed different cell clusters, which might reflect either different cell types or different phenotypes of microglia cells. These cell clusters were therefore analyzed separately. In this context, it needs to be critically considered that peripheral immune cells might have crossed the blood-brain-barrier due to epilepsy-associated alterations compromising the barrier function [3,33–35]. This might have marginally affected the outcome of ROS generation in the performed analysis.

A limitation of our study might be that we had to pool three whole brains per experiment to gain sufficient cell yields. The dilution effect might have contributed to the lack of alterations in the chronic phase.

In conclusion, we were able to demonstrate that microglial ROS generation in the time course of epileptogenesis reaches a peak after the initial insult, is only marginally increased in the latency phase and returns to control levels during the chronic epileptic phase in the electrical rat post-SE model.

The time course of microglial ROS generation suggests that the application of combined anti-inflammatory and radical scavenging approaches might only be beneficial, when applied during a short critical time window after an epileptogenic brain insult.

Conflict of interest

All authors disclose any actual or potential conflict of interest including any financial, personal or other relationships with other people or organizations within three years of beginning the submitted work that could inappropriately influence, or be perceived to influence, their work.

Acknowledgements

Appendix A. Supplementary data

Supplementary data associated with this article can be found, in the online version, at http://dx.doi.org/10.1016/j.neulet.2015.05.041

References

[1] S. Waldbaum, M. Patel, Mitochondrial dysfunction and oxidative stress: a contributing link to acquired epilepsy, J. Bioenerg. Biomembr. 42 (6) (2010) 449–455.

[2] A. Vezzani, A.R.J. Friedman Dingledine, The role of inflammation in epileptogenesis, Neuropharmacology 69 (2013) 16–24.

[3] H. Kettenmann, et al., Physiology of microglia, Physiol. Rev. 91 (2) (2011) 461–553.

[4] W. Löscher, C. Brandt, Prevention or modification of epileptogenesis after brain insults: experimental approaches and translational research, Pharmacol. Rev. 62 (4) (2010) 668–700.

[5] S. Waldbaum, M. Patel, Mitochondria, oxidative stress, and temporal lobe epilepsy, Epilepsy Res. 88 (1) (2010) 23–45.

[6] M. Atanasova, et al., Strain-dependent effects of long-term treatment with melatonin on kainic acid-induced status epilepticus, oxidative stress and the expression of heat shock proteins, Pharmacol. Biochem. Behav. 111 (2013) 44–50.

[7] L.P. Liang, Y.S.M. Ho Patel, Mitochondrial superoxide production in kainate-induced hippocampal damage, Neuroscience 101 (3) (2000) 563–570.

[8] L.P. Liang, M. Patel, Seizure-induced changes in mitochondrial redox status, Free Radic. Biol. Med. 40 (2) (2006) 316–322.

[9] K. Ryan, et al., Temporal and spatial increase of reactive nitrogen species in the kainate model of temporal lobe epilepsy, Neurobiol. Dis. 64 (2014) 8–15.

[10] A. Emmendörffer, et al., A fast and easy method to determine the production of reactive oxygen intermediates by human and murine phagocytes using dihydrorhodamine 123, J. Immunol. Methods 131 (2) (1990) 269–275.

[11] V.M. Stein, et al., Characterization of canine microglial cells isolated ex vivo, Vet. Immunol. Immunopathol. 99 (1–2) (2004) 73–85.

[12] A. Pekcec, et al., Impact of the PSA-NCAM system on pathophysiology in a chronic rodent model of temporal lobe epilepsy, Neurobiol. Dis. 27 (1) (2007) 54–66.

[13] T. Ongerth, et al., Targeting of microglial K3. 1 channels by TRAM-34 exacerbates hippocampal neurodegeneration and does not affect ictogenesis and epileptogenesis in chronic temporal lobe epilepsy models, Eur. J. Pharmacol. 740C (2014) 72–80.

[14] A. Pekcec, et al., Targeting epileptogenesis-associated induction of neurogenesis by enzymatic depolysialylation of NCAM counteracts spatial learning dysfunction but fails to impact epilepsy development, J Neurochem 105 (2) (2008) 389–400.

[15] A.L. Ford, et al., Normal adult ramified microglia separated from other central nervous system macrophages by flow cytometric sorting. Phenotypic differences defined and direct ex vivo antigen presentation to myelin basic protein-reactive CD4+T cells compared, J. Immunol. 154 (9) (1995) 4309–4321.

[16] J.D. Sedgwick, et al., Isolation and direct characterization of resident microglial cells from the normal and inflamed central nervous system, Proc. Natl. Acad. Sci. U. S. A. 88 (16) (1991) 7438–7442.

[17] V.M. Stein, et al., Characterization of canine microglial cells isolated ex vivo, Vet. Immunol. Immunopathol. 99 (1–2) (2004) 73–85.

[18] H. Kato, et al., Progressive expression of immunomolecules on activated microglia and invading leukocytes following focal cerebral ischemia in the rat, Brain Res. 734 (1–2) (1996) 203–212.

[19] H. Akiyama, P.L. McGeer, Brain microglia constitutively express β-2 integrins, J. Neuroimmunol. 30 (1) (1990) 81–93.

[20] M. Naziroglu, Role of selenium on calcium signaling and oxidative stress-induced molecular pathways in epilepsy, Neurochem. Res. 34 (12) (2009) 2181–2191.

[21] S. Rowley, M. Patel, Mitochondrial involvement and oxidative stress in temporal lobe epilepsy, Free Radic. Biol. Med. 62 (2013) 121–131.

[22] M. Penkowa, et al., Interleukin-6 deficiency reduces the brain inflammatory response and increases oxidative stress and neurodegeneration after kainic acid-induced seizures, Neuroscience 102 (4) (2001) 805–818.

[23] T. Schilling, C. Eder, Stimulus-dependent requirement of ion channels for microglial NADPH oxidase-mediated production of reactive oxygen species, J. Neuroimmunol. 225 (1–2) (2010) 190–194.

[24] H. Sleven, et al., Depletion of reduced glutathione precedes inactivation of mitochondrial enzymes following limbic status epilepticus in the rat hippocampus, Neurochem. Int. 48 (2) (2006) 75–82.

[25] F. Dal-Pizzol, et al., Lipid peroxidation in hippocampus early and late after status epilepticus induced by pilocarpine or kainic acid in Wistar rats, Neurosci. Lett. 291 (3) (2000) 179–182.

[26] M. Levesque, M. Avoli, The kainic acid model of temporal lobe epilepsy, Neurosci. Biobehav. Rev. 37(10 Pt 2) (2013) 2887–2899.

[27] K.T. Kishida, E. Klann, Sources and targets of reactive oxygen species in synaptic plasticity and memory, Antioxid. Redox Sign. 9 (2) (2007) 233–244.

[28] A. Vezzani, T.Z. Baram, New roles for interleukin-1 beta in the mechanisms of epilepsy, Epilepsy Curr. 7 (2) (2007) 45–50.

[29] B.S. Meldrum, Concept of activity-induced cell death in epilepsy: historical and contemporary perspectives, in: A.P. Thomas Sutula (Ed.), Progress in Brain Research, Elsevier, 2002, pp. 3–11.

[30] J. Folbergrova, Oxidative stress in immature brain following experimentally-induced seizures, Physiol. Res. 62 (Suppl. 1) (2013) S39–48.

[31] M. Schwartz, et al., Microglial phenotype: is the commitment reversible? Trends Neurosci. 29 (2) (2006) 68–74.

[32] F. Gonzalez-Scarano, G. Baltuch, Microglia as mediators of inflammatory and degenerative diseases, Annu. Rev. Neurosci. 22 (1999) 219–240.

[33] M. Zattoni, et al., Brain infiltration of leukocytes contributes to the pathophysiology of temporal lobe epilepsy, J. Neurosci. 31 (11) (2011) 4037–4050.

[34] T. Ravizza, et al., Innate and adaptive immunity during epileptogenesis and spontaneous seizures: evidence from experimental models and human temporal lobe epilepsy, Neurobiol. Dis. 29 (1) (2008) 142–160.

[35] N.C. Manley, et al., Characterization of monocyte chemoattractant protein-1 expression following a kainate model of status epilepticus, Brain Res. 1182 (2007) 138–143.